Self-Assembly of CdSe−ZnS Quantum Dot Bioconjugates Using an Engineered Recombinant Protein

Hedi Mattoussi,*,† J. Matthew Mauro,‡ Ellen R. Goldman,§ George P. Anderson,‡ Vikram C. Sundar,⊥ Frederic V. Mikulec,⊥ and Moungi G. Bawendi⊥

Contribution from the Optical Sciences Division, Code 5611, Center for Bio/Molecular Science and Engineering, Code 6900, United States Naval Research Laboratory, Washington, D.C. 20375, Georgetown University Medical Center, Department of Biochemistry and Molecular Biology, Washington D.C. 20007, and Center for Materials Science and Engineering and Department of Chemistry, Massachusetts Institute of Technology, Cambridge, Massachusetts 02139

Received July 12, 2000

Abstract: A novel and direct method is described for conjugating protein molecules to luminescent CdSe−ZnS core−shell nanocrystals (Quantum Dots) for use as bioactive fluorescent probes in sensing, imaging, immunoassay, and other diagnostics applications. The approach makes use of a chimeric fusion protein designed to electrostatically bind to the oppositely charged surface of capped colloidal quantum dots (QDs). Preparation of protein-modified QD dispersions with high quantum yield, little or no particle aggregation, and retention of biological activity was achieved. Combining the advantages of lipoic acid capped CdSe−ZnS quantum dots (photochemical stability, a wide range of size-dependent emission wavelengths, and aqueous compatibility) with facile electrostatic conjugation of bioactive proteins, this type of hybrid bioinorganic conjugate represents a powerful fluorescent tracking tool for diverse applications. The design and preparation of a model QD/protein conjugate based on *E. coli* Maltose Binding Protein is described, together with functional characterization of this new type of nanoassembly using luminescence, laser scanning microscopy, and bioassay.

Introduction and Background

Labeling of biological molecules using fluorescent tags is a common and very useful practice in biological science. Fluorescent small molecules (organic dyes) are used in both single and multiplex detection approaches.[1,2] However, tagging of biomolecules using organic fluorophores has significant limitations. Organic fluorophores tend to have narrow excitation spectra, and often exhibit broad emission bands with red tailing, which makes simultaneous quantitative evaluation of relative amounts of different probes present in the same sample difficult, due to spectral overlap.[3] Furthermore, variation of the absorption and/or emission spectra of dye tagged bioconjugates requires the use of chemically distinct molecular labels with attendant synthesis and conjugation challenges. Nonetheless, the use of multiple dye labels has achieved a considerable level of sophistication, as demonstrated by recent flow cytometry work involving a three-laser system and eight-color-marking scheme to simultaneously measure a total of 10 parameters on cellular antigens.[2]

Colloidal semiconductor nanocrystals, often referred to as "quantum dots" or "QDs", have the potential to overcome problems encountered by organic small molecules in certain fluorescent tagging applications by combining the advantages of high photobleaching threshold, good chemical stability, and readily tunable spectral properties. During routine preparation, their inorganic core is capped with an organic layer such as a trioctyl phosphine/trioctyl phosphine oxide mixture (TOP/TOPO). Substitution of this organic cap with other appropriate groups (cap exchange) permits tailoring of nanoparticles for efficient dispersal in various organic solvents. Replacing the TOP/TOPO cap with polar terminated groups allows dispersal of these nanoparticles in aqueous solutions with preservation of a high photoluminescence (PL) quantum yield. For example, using dihydrolipoic acid capping groups allows preparation of stable aqueous dispersions of CdSe−ZnS core−shell nanocrystals with quantum yields of 10−20%.

Colloidal quantum dots used most often to date in fundamental or applied studies are spherical nanocrystals with core sizes that vary between 15 and 120 Å in diameter.[4,5,6] Their optical and electronic properties are dominated by carrier confinement (electron/hole), which results in size dependence of their optical properties, including light absorption, PL, electroluminescence (EL),[7−11] and cathodoluminescence (CL).[12,13]

* To whom correspondence should be addressed.
† Optical Sciences Division, United States Naval Research Laboratory.
‡ Center for Bio/Molecular Science and Engineering, United States Naval Research Laboratory.
§ Georgetown University.
⊥ Massachusetts Institute of Technology.

(1) Schröck, E.; du Manoir, S.; Veldman, T.; Schoell, B.; Wienberg, J.; Ferguson-Smith, M. A.; Ning, Y.; Ledbetter, D. H.; Bar-Am, I.; Soenksen, D.; Garini, Y.; Ried, T. *Science* **1996**, 273, 494−497.
(2) Roederer, M.; DeRosa, S.; Gerstein, R.; Anderson, M.; Bigos, M.; Stovel, R.; Nozaki, T.; Parks, D.; Herzenberg, L.; Herzenberg, L. *Cytometry* **1997**, *29*, 328−339.
(3) Hermanson, G. T. *Bioconjugate Techniques*; Academic Press: London, UK, 1996; Chapter 8 and references therein.
(4) Murray, C. B.; Norris, D. J.; Bawendi, M. G. *J. Am. Chem. Soc.* **1993**, *115*, 8706−8715.
(5) Mattoussi, H.; Cumming, A. W.; Murray, C. B.; Bawendi, M. G.; Ober, R. *J. Chem. Phys.* **1996**, *105*, 9890−9896.
(6) Mattoussi, H.; Cumming, A. W.; Murray, C. B.; Bawendi, M. G.; Ober, R. *Phys. Rev.* **1998**, *B58*, 7850−7863.
(7) Colvin, V. L.; Schlamp, M. C.; Alivisatos, A. P. *Nature* **1994**, *370*, 354−356.
(8) Dabbousi, B. O.; Bawendi, M. G.; Onitsuka, O.; Rubner, M. F. *Appl. Phys. Lett.* **1995**, *66*, 1316−1318.
(9) Schlamp, M. C.; Peng, X. G.; Alivisatos, A. P. *J. Appl. Phys*. **1997**, *82*, 5837−5842.

10.1021/ja002535y CCC: $19.00
Published on Web 11/22/2000

Nanocrystals composed of ZnSe, CdS, CdSe, and CdTe have emission spectra that span the visible spectrum.[4,14−16] Nanocrystals made of other materials (e.g., InAs, InP, and PbS) have photoluminescent emission that extends into the near-IR[17−19]

CdSe nanocrystals have broad absorption spectra with a first absorption peak (band edge) that progressively shifts to longer wavelengths with increasing particle size. Their PL spectra are narrow (full width at half-maximum, fwhm, of ∼25−40 nm), and their emission positions track the absorption band edge location, spanning the visible spectrum. These nanocrystals are thus tunable fluorophores with absorption characteristics that allow simultaneous excitation of different particle sizes at a single wavelength, while they exhibit a luminescent emission that spans a wide range of wavelengths in the visible spectrum. Overcoating the CdSe core with a wider band gap semiconducting material such as ZnS or CdS, a process based on the concepts of band-gap engineering used in electronics, permits passivation of surface states and reduces the leakage of excitons outside the core.[20−22] This enhances the photochemical stability and resistance to photobleaching of these nanomaterials. Overcoating also improves the luminescence quantum yield substantially without affecting the location or spectral bandwidth of light emission, i.e., CdSe−ZnS nanoparticles have an emission fwhm of ∼30−45 nm.[21]

The above QD luminescence properties suggest the possibility of considerable sensitivity in fluorescent detection applications. Figure 1 shows a plot of the dependence of integrated PL intensity versus dilution factor (or nanoparticle concentration), along with two representative emission spectra at the lowest examined concentrations of CdSe−ZnS QDs in hexane. Substantial PL integrated intensities with good signal-to-noise ratios and well-resolved emission spectra are measured for nanoparticle dispersions with concentrations smaller than 1 nmol of particles per liter. This is comparable to the sensitivity reached in similar conditions with the best conventional organic fluorophores.

The wide range of useful size-dependent excitation and emission wavelengths of these materials, their resistance to photobleaching, along with their high quantum yield in aqueous solutions make them attractive for labeling functional biomolecules for fluorescent tagging applications. Experiments involving labeling of metallic and/or magnetic nanocrystals having organic capping molecules on their surfaces have been reported,[23−25] and there have been two important studies utilizing CdSe nanocrystals bound to biological molecules.[26,27] In one study, an avidin−biotin binding scheme was employed to attach CdSe−CdS core−shell nanoparticles to actin fibers. These dots were capped with an additional thin layer of derivatized porous silica, to render them water compatible. The route to the final conjugate was complex and time-consuming, and yielded a product with a relatively low quantum yield.[26] Furthermore, it must be carried out at extremely dilute conditions, which means that the amount of material obtained is inherently limited. The second study used CdSe−ZnS core−shell nanoparticles capped with mercaptoacetic acid groups. In this case, a conventional covalent cross-linking approach based on 1-ethyl-3-(3-dimethylaminopropyl) carbodiimide hydrochloride (EDC) condensation was used to conjugate the nanoparticles to immunoglobulin G (IgG).[28] Successful preparation of QD/IgG conjugates was reported, albeit again with low PL quantum yields.[27] A more recent study reported immobilization of thiol-terminated DNA segments (20−25-mers) on mercaptopropionic acid capped CdSe−ZnS nanocrystals. The resulting DNA-modified QDs were subsequently used to build hybrid assemblies with DNA-modified gold nanocrystals.[29] In this case, binding of DNA segments to the QDs was driven by favorable interactions between thiol groups and the inorganic surface, similar to what has been reported for gold particles. In another report, interactions of polynucleotides, such as DNA, with quantum dots induced quenching in the luminescence emission of 40-Å CdS nanocrystals.[30]

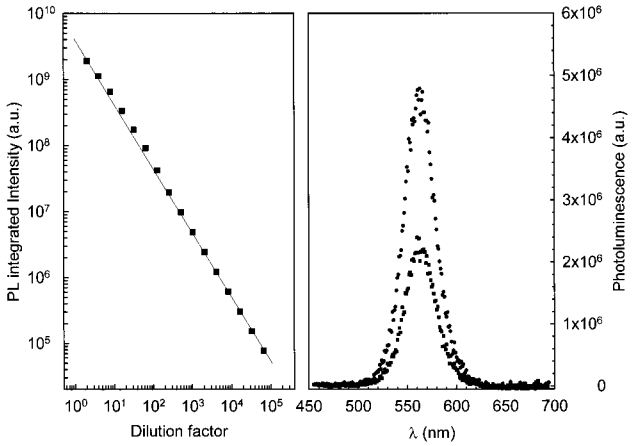

Figure 1. Left panel: Plot of integrated photoluminescence signal versus concentration covering 5 decades of dilution of CdSe−ZnS in hexane. The nominal particle core radius R_0 was 19 Å. Concentrations examined range from 0.395 μmol/L to 50 pmol/L. Samples were excited at 350 nm and PL data were collected using a 10 mm optical path cell. Right panel: PL spectra of two representative dilute QD solutions at ∼13 nmol/L (●) and at ∼6.5 nmol/L (■). Well-resolved spectra with high signal-to-noise ratios were obtained for concentrations as low as 10 pmol/L.

Our attempts to covalently attach proteins to CdSe−ZnS nanoparticles capped with dihydrolipoic acid groups using EDC were relatively unsuccessful. With either immunoglobulin G (IgG) or ovalbumin these experiments consistently resulted in the formation of a high level of extensively aggregated dot/protein conjugates in the preparations. We therefore developed an alternative conjugation strategy, based on self-assembly utilizing electrostatic attractions between negatively charged lipoic acid capped CdSe−ZnS quantum dots and engineered bifunctional recombinant proteins consisting of positively

(10) Mattoussi, H.; Radzilowski, L. H.; Dabbousi, B. O.; Thomas, E. L.; Bawendi, M. G.; Rubner, M. F. *J. Appl. Phys.* **1998**, *83*, 7965−7974.
(11) Mattoussi, H.; Radzilowski, L. H.; Dabbousi, B. O.; Fogg, D. E.; Schrock, R. R.; Thomas, E. L.; Rubner, M. F.; Bawendi, M. G. *J. Appl. Phys.* **1999**, *86*, 4390−4399.
(12) Rodriguez-Viejo, J.; Jensen, K. F.; Mattoussi, H.; Michel, J.; Dabbousi, B. O.; Bawendi, M. G. *Appl. Phys. Lett.* **1997**, *70*, 2132−2134.
(13) Rodriguez-Viejo, J.; Mattoussi, H.; Heine, J. R.; Kuno, M. K.; Michel, J.; Bawendi, M. G.; Jensen, K. F. *J. Appl. Phys.* **2000**, *87*, 8526−8534.
(14) Steigerwald, M. L.; Alivisatos, A. P.; Gibson, J. M.; Harris, T. D.; Kortan, R.; Muller, A. J.; Thayer, A. M.; Duncan, T. M.; Douglass, D. C.; Brus, L. E. *J. Am. Chem. Soc.* **1988**, *110*, 3046−3050.
(15) Hines, M. A.; Guyot-Sionnest, P. *J. Phys Chem.* **1998**, *B102*, 3655−3657.
(16) Mikulec, F. V. Ph.D. dissertation, Massachusetts Institute of Technology, 1999.
(17) Guzelian, A. A.; Banin, U.; Kadavanich, A. V.; Peng, X. G.; Alivisatos, A. P. *Appl. Phys. Lett.* **1996**, *69*, 1432−1434.
(18) Wundke, K.; Potting, S.; Auxier, J.; Schulzgen, A.; Peyghambarian, N.; Borrelli, N. F. *Appl. Phys. Lett.* **2000**, *76*, 10−12.
(19) Guerreiro, P. T.; Ten, S.; Borrelli, N. F.; Butty, J.; Jabbour, G. E.; Peyghambarian, N. *Appl. Phys. Lett.* **1997**, *71*, 1595−1597.
(20) Hines, M. A.; Guyot-Sionnest, P. *J. Phys. Chem.* **1996**, *100*, 468−471.
(21) Dabbousi, B. O.; Rodrigez-Viejo, J.; Mikulec, F. V.; Heine, J. R.; Mattoussi, H.; Ober, R.; Jensen, K. J.; Bawendi, M. G. *J. Phys. Chem.* **1997**, *101*, 9463−9475.
(22) Peng, X. G.; Schlamp, M. C.; Kadavanich, A. V.; Alivisatos, A. P. *J. Am. Chem. Soc.* **1997**, *119*, 7019−7029.

charged attachment domains (containing a leucine zipper) genetically fused with desired biologically relevant domains.

The strategy of combining the use of alkyl-COOH capped CdSe−ZnS nanocrystals and two-domain recombinant proteins cloned with a highly charged leucine zipper tail offers several advantages. (1) The alkyl-COOH terminated capping groups, which permit dispersion of the nanocrystals in water solutions at basic pH, also provide a surface charge distribution that can promote direct self-assembly with other molecules that have a net positive charge. (2) The synthetic approach used to prepare the QDs can be easily applied to a number of different core−shell nanocrystals and extended to other combinations of semiconducting materials, II−VI and III−V, which can generate a group of fluorescent probes with tunable emission over a wide range of wavelengths. This contrasts with the need for developing specific chemistry routes for each organic fluorescent dye case by case. (3) The fusion protein approach provides a general and consistent way to prepare a wide selection of biological macromolecules amenable to alterations of the interaction domain, such as charge, size, stability to pH, and temperature. This also allows control of the assembly of individual proteins, e.g., into monomers, dimers, and tetramers, a property that can be exploited in protein packing around the nanocrystals to form complex bioconjugates. In the present report we describe the design, preparation, and initial analysis of a model QD/protein conjugate based on this strategy.

Experimental Section

(a) Preparation of Water-Soluble CdSe−ZnS Core−Shell Nanoparticles. Water-soluble CdSe−ZnS nanoparticles, compatible with aqueous conjugation conditions, were prepared using a stepwise procedure consisting of core nanocrystal growth, ZnS overcoating, TOP/TOPO-capping and size selection precipitation, dihydrolipoic acid cap exchange, and final washing/cleaning. TOP/TOPO-capped CdSe−ZnS core−shell particles were prepared using the previously described synthesis route based on growth and annealing of organometallic compounds at high temperature.[4,20,21] A relatively thick ZnS overcoating of 5−7 monolayers was used.[21] TOP/TOPO capping groups were subsequently exchanged with dihydrolipoic acid groups by suspending 100−300 mg of TOP/TOPO-capped dots after size selection precipitation in 150−500 μL of dihydrolipoic acid (freshly prepared from distilled thioctic acid [Aldrich] by borohydride reduction).[31] The mixture was heated to ∼60−70 °C and let stand for several hours. After dilution with ∼1.5 mL of dimethylformamide (DMF), deprotonation of the terminal lipoic acid −COOH groups was carried out by slowly adding excess potassium *tert*-butoxide, about 5 times the mass of the initial quantum dots used. The resulting precipitate consisting of the nanoparticles together with released TOP/TOPO reagents was sedimented by centrifugation. The sedimented precipitate was then dispersed in water, but in some cases solution was slightly turbid because of unremoved TOP/TOPO molecules. Centrifugation or filtration of the dispersion (using a 0.5 μm disposable filter) permitted removal of the TOP/TOPO and provided a clear dispersion of the alkyl-COOH capped nanocrystals. The nanoparticle dispersion was further separated from excess hydrolyzed potassium *tert*-butoxide and residual DMF by 4 cycles of concentration/dilution (10:1), using an Ultra-free centrifugal filtration device (Millipore, M_W cutoff of ∼50000 daltons), and redispersed in water. The final clean and stable aqueous QD dispersions had the emission characteristics of the initial nanocrystals and a PL yield of ∼10−20%. Dispersions of QDs in aqueous suspension with dot concentrations of ∼5 to 30 μM were prepared and stored for future use. Nanoparticle concentrations were estimated from measurements of the integrated absorption spectrum (over the range 350−700 nm) and comparing the value to that of the growth solution measured shortly after preparation.[21,32] The present polar-capped, negatively charged QDs are stable and have useful luminescence emission only in very weakly acidic or buffered basic solutions (i.e., pH >6). More acidic solutions induce macroscopic precipitation of the nanoparticles along with a substantial loss in the PL emission, due to loss of surface charge upon cap protonation and/or loss of cap affinity for the ZnS overcoat.

(b) Cloning and Preparation of the Maltose Binding Protein-Basic Leucine Zipper (MBP-zb) Fusion Protein. The coding DNA sequence for the two-domain model Maltose Binding Protein-basic zipper fusion protein (MBP-zb) was constructed using standard gene assembly and cloning techniques. A cartoon representing the idealized MBP-zb dimer and the detailed nucleotide coding and primary amino acid sequences is shown in Figure 2b.

Two DNA primers were synthesized to anneal to the 5′ and 3′ ends of the basic leucine zipper in the pCRIIBasic plasmid kindly supplied by H. C. Chang of Harvard University.[33]

primer 1: 5′-TGCGGTGGCTCAGCTCAGTTG-3′

primer 2: 5′-GCTCTAGATTAATCCCCACCCT
GGGCGAGTTTC-3′

Using 25 cycles of PCR (30 s at 94 °C, 90 s at 60 °C, and 90 s at 72 °C) the basic zipper DNA sequence was amplified using primers 1 and 2 and pfu DNA polymerase (Stratagene) to produce a 174 bp DNA fragment coding for the basic zipper as designed by O'Shea et al.[34] and previously successfully employed in a recombinant system by Chang et al. for formation of T-cell receptor dimers.[33] Digestion of this amplified DNA with XbaI endonuclease yielded a fragment with termini suitable for forced ligation into the XmnI/XbaI sites within the polylinker that exists downstream of the MalE gene in the commercially obtained pMal-c2 vector [New England Biolabs]. The coding sequence for a C-terminal TAA translation stop codon and a unique cysteine residue upstream of the basic leucine zipper sequence was also incorporated during PCR amplification using these primers. After transformation of *E. coli* DH5α with ligation products and analyzing several ampicillin resistant transformants by colony PCR using analytical oligonucleotide primers annealing to the pMal-c2 vector DNA sequence flanking the cloned insert, pMBP-zb plasmid DNA was prepared from an overnight growth on a 10 mL scale. The correct expected nucleotide sequence for the basic leucine zipper in the new clone pMBP-zb was verified for this plasmid DNA by the MGIF sequencing facility at the University of Georgia. Small-scale expression studies in several bacterial strains were subsequently conducted to optimize production of the fusion protein. *E. coli* BL21, a protease deficient strain, proved to be most suitable for liter scale cell culture and expression of MBP-zb protein.

Cells were cultured for a typical preparation of MBP-zb by inoculation of 10 mL of Luria Broth (LB) containing 100 μg/mL of carbenicillin with a single colony of freshly transformed *E. coli* BL21. The starter culture was shaken at 37 °C overnight (ca. 15 h). A 0.50 mL sample of this overnight culture was transferred into 250 mL of LB containing 50 μg/mL of carbenicillin and 2 g of glucose/L. After growing to an optical density of ca. 0.8 at 37 °C, the flask containing

(23) Hermanson, G. T. *Bioconjugate Techniques*; Academic Press: London, UK, 1996; Chapter 14 and references therein.
(24) Eychmuller, A.; Mews, A.; Weller, H. *Chem. Phys. Lett.* **1993**, *208*, 59−62.
(25) Elghanian, R.; Storhoff, J. J.; Mucic, R. C.; Letsinger, R. L.; Mirkin, C. A. *Science* **1997**, *277*, 1078−1081.
(26) Bruchez, M., Jr.; Moronne, M.; Gin, P.; Weiss, S.; Alivisatos, A. P. *Science* **1998**, *281*, 2013−2016.
(27) Chan, W. C. W.; Nie, S. *Science* **1998**, *281*, 2016−2018.
(28) Hermanson, G. T. *Bioconjugate Techniques*; Academic Press: London, UK, 1996; Chapter 3 and references therein.
(29) Mitchell, G. P.; Mirkin,C. A.; Letsinger, R. L. *J. Am. Chem. Soc.* **1999**, *121*, 8122−8123.
(30) Bigham, S. R.; Coffer, J. L. *J. Phys. Chem.* **1992**, *96*, 10581−10584.
(31) Gunsalus, I. C.; Barton, L. S.; Gruber, W. *J. Am. Chem. Soc.* **1956**, *78*, 1763−1768.
(32) Dabbousi, B. O. Ph.D. dissertation, Massachusetts Institute of Technology, 1997.
(33) Chang, H. C.; Bao, Z.; Yao, Y.; Yse, A. G.; Goyarts, E. C.; Madsen, M.; Kawasaki, E.; Brauer, P. P.; Sacchattini, J. C.; Nathenson, S. G.; Reinherz, E. L. *Proc. Natl. Acad. Sci. U.S.A.* **1994**, *91*, 11408−11412.
(34) O'Shea, E. K.; Lumb, K. J.; Kim, P. S. *Curr. Biol.* **1993**, *3*, 658−667 and references therein.

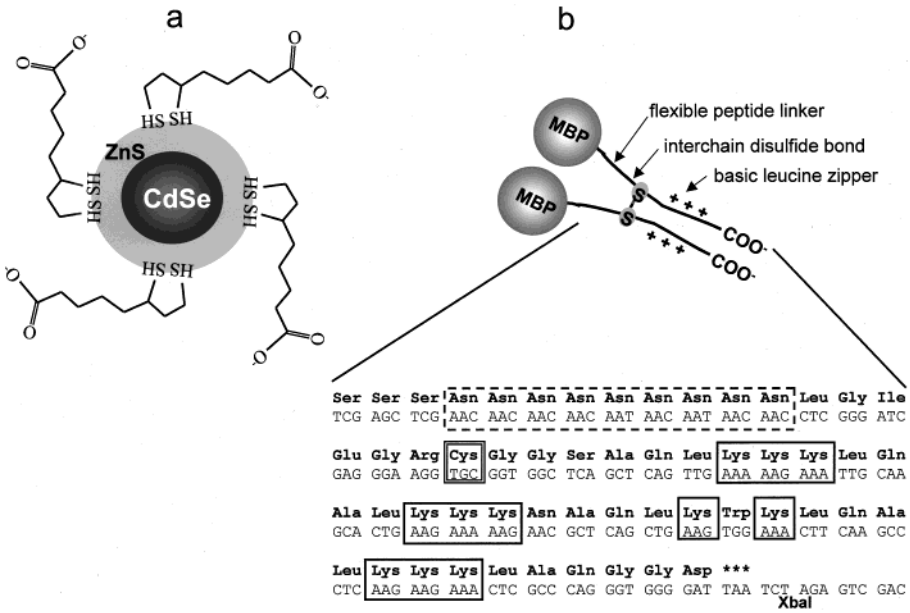

Figure 2. (a) Schematic of the CdSe−ZnS core−shell nanoparticle with dihydrolipoic acid surface capping groups; (b) cartoon of the S−S linked MBP-zb homodimer and detail showing nucleotide and primary amino acid sequences of the C-terminal basic leucine zipper interaction domain. Poly-Asn flexible linker is boxed with dashed lines, unique engineered cysteine is double boxed, and lysine residues contributing to net positive charge of leucine zipper are single boxed.

the cell culture was shaken at 30 °C for 15 min prior to adding IPTG (isopropylthiogalactopyranoside) to a final concentration of 1 mM. After 2 h at this temperature, the cells were sedimented at 4 °C by centrifugation. The resulting cell pellet was quick frozen in powdered dry ice and stored at −80 °C until thawing for purification.

Affinity purification of MBP-zb was accomplished by amylose affinity chromatography with minor modifications in the procedures described in New England Biolabs' Protein Fusion and Purification System product literature. Briefly, the thawed bacterial pellet from 250 mL of culture was resuspended in 7 mL of 20 mM HEPES, 300 mM NaCl (pH 7.4) to which one tablet of Boehringer mini-complete (+EDTA) protease inhibitor cocktail had been freshly dissolved. The cell suspension was sonicated 5 × 30 s (Bransonic 450; microtip) on ice. After centrifugation for 30 min at 14000×g (4 °C), the supernate was diluted with an equal volume of lysis buffer prior to loading onto a 10 mL column of amylose affinity matrix (New England Biolabs) previously equilibrated at 4 °C in lysis buffer (without protease inhibitors). The adsorbed sample on the column was washed with 50 mL of buffer and then eluted with the same buffer containing 10 mM maltose (Sigma). Eluted fractions were analyzed by reducing/denaturing SDS gel electrophoresis on 8/25% Phast gels (Pharmacia) and Coomassie Brilliant Blue R staining. Appropriate fractions were pooled (protein concentration of ∼3 mg/mL ∼ 100 μM) and stored at 4 °C for one week to allow spontaneous intermolecular disulfide bond formation to occur. Covalent dimerization via S−S bonds was verified to be at least 90% complete after this time interval by gel electrophoresis analysis conducted both with and without 30 mg/mL of dithiothreitol (Sigma) reducing agent in heated SDS denatured samples.

Maltose eluent was removed from affinity-purified dimerized MBP-zb by gel permeation chromatography at room temperature using BioGel P10 matrix (Bio-Rad) previously equilibrated with buffer appropriate for QD bioconjugation experiments. Purified maltose-free MBP-zb stored at a concentration of 1−3 mg/mL (4 °C) remained functionally unchanged for at least a year. Protein concentrations were measured using the BCA Protein Assay (Pierce) method.

c. QD/MBP-zb Conjugate Preparation and Analysis Techniques. Conjugation of lipoic acid capped core−shell nanoparticles with MBP-zb protein was carried out in 5 mM sodium borate at pH 9. In all experiments, simply mixing dissolved fusion protein with QD nanoparticle material in buffered media yielded self-assembled QD/protein conjugates ready for testing within a few minutes. The resulting preparations contained stable QD/MBP-zb conjugates free of obvious sedimentable aggregates.

Laser scanning confocal microscopy images were collected using a Leica TCS SP microscope (from Leica Microsystems Heidelberg GmbH), with excitation at 488 nm. Liquid dot films for observation (1−2 mm final thickness) were prepared by spreading a few drops of the suspensions on the surface of an optical dish mounted on the microscope stage. The excitation beam was vertically propagated (z direction in Figure 3) and images representing luminescence emission of defined-thickness horizontal cross-sections ($x-y$ plane in Figure 3) were collected over a scanning time of ∼0.1−0.5 s per image. Each image corresponded to a scan over an area of 19.60 μm × 11.75 μm and 14.6-μm thick cross-section, with the exact image size determined by microscope objective and focusing parameters. Signal collection time was optimized for best contrast.

Absorption spectra were collected using a diode array UV−vis spectrometer HP8453 (Hewlett-Packard). PL emission spectra were collected using a SPEX Fluorolog 3 (ISA). In both experiments 10 mm optical path cells (from Spectrocell) were used to collect the absorption and PL spectra.

Displacement titration of QD/MBP-zb conjugates pre-bound to amylose affinity resin by maltose was carried out by first adding 100 μL of a suspension of resin-bound QD/MBP-zb to each of a set of filter wells in a porous-bottom microtiter plate (3 μm pore size; Pall Corp.). Increasing amounts of maltose were then added to the wells, resulting in displacement from the affinity resin of a fraction of the QD/MBP-zb bioconjugates in each well depending on the final concentration of maltose. After an equilibration period of 30 min the suspensions were pressure filtered to separate displaced conjugates from material that remained bound to the amylose beads. PL emission of QD/MBP-zb remaining bound to resin was measured using a Spectra Fluor Plus microtiter plate reader (Tecan). A 25-nm band-pass filter was used for excitation at 360 nm and a long pass filter with a cutoff at 530 nm was used for monitoring the PL intensity. Experiments to measure the effects of ionic strength on the photoluminescence from dispersions of QDs and QD/protein conjugates were also carried out using a microtiter plate and the above Spectra Fluor Plus plate reader.

Results

Figure 3 presents a set of laser scanning confocal microscopy images of dispersions of nanoparticle and nanoparticle/protein conjugate populations (average particle core CdSe radius of ∼19 Å). Images of unconjugated lipoic acid capped dots (Figure 3a), dots conjugated with MBP-zb using the present approach (Figure

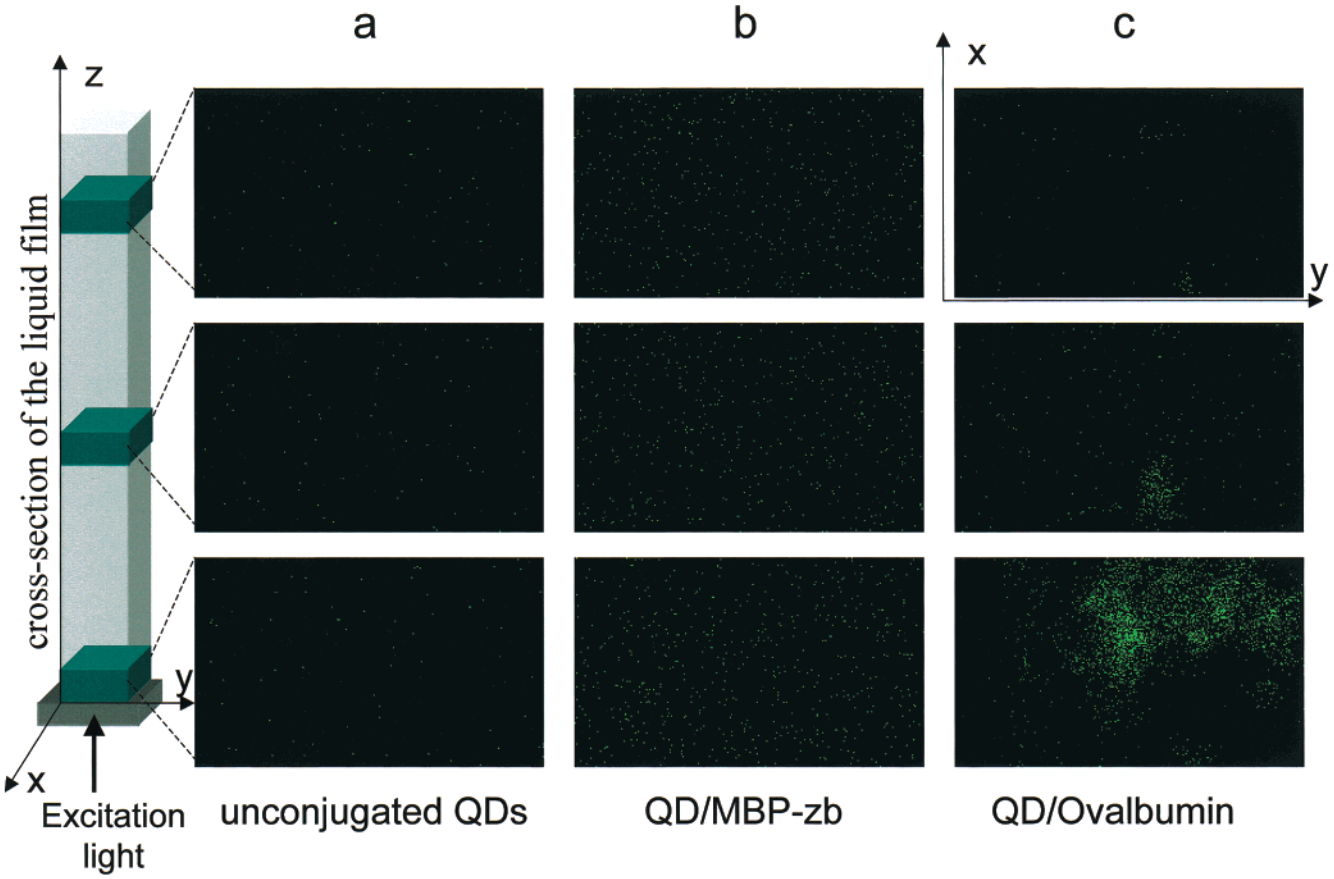

Figure 3. Laser scanning fluorescence images of cross-sectional slices along the *z* direction for three aqueous samples: (a) unconjugated quantum dots; (b) QD/MBP-zb bioconjugates; and (c) QD/ovalbumin conjugates prepared using the EDC approach. A sketch of the solution film cross-section is shown at left. Each image represents a cross-section of 19.60 μm × 11.75 μm and a thickness of ∼14.6 μm. MBP-zb conjugates were prepared at a MBP-zb:QD molar ratio of 14:1.

3b), and the same nanoparticles conjugated with ovalbumin using the covalent EDC labeling approach (Figure 3c) are shown. The images represent the luminescence emission from thin cross-sections (∼14.6 μm thick and an area of 19.60 μm × 11.75 μm each) along the excitation path. The lower-most images in Figure 3 represent cross-sections directly adjacent to the support surface (bottom of the optical dish). Each bright point represents emission from an individual nanoparticle center within the cross-sections in samples a and b. These images are essentially identical to the features of those observed in previous single dot spectroscopy.[35,36] Images taken from dispersions of nanoparticles conjugated with MBP-zb show luminescent centers homogeneously distributed over each cross-section. These are very similar to images of dispersions of unconjugated nanoparticles; however, a substantially higher density of luminescent centers is observed for the sample containing an identical concentration of MBP-zb conjugated dots, due to the larger quantum yield of the conjugated nanoparticles (see below, Figure 4).[35] Notably, there were no obvious heavy aggregates settled onto the optical dish surface, demonstrating that effective formation of QD conjugates with little or no aggregation had occurred. These preparations (containing dots plus MBP-zb) are stable for at least several months when stored at 4 °C.

In contrast, images taken from dispersions containing dots that were covalently conjugated with ovalbumin using EDC showed only very small numbers of discrete homogeneously distributed emission centers (bright spots) in sections scanned above the bottom surface. The lowest layer observed, directly adjacent to the support surface, showed large amounts of aggregated material. Aggregation was even more pronounced in trials where IgG was conjugated to the QDs via EDC condensation.

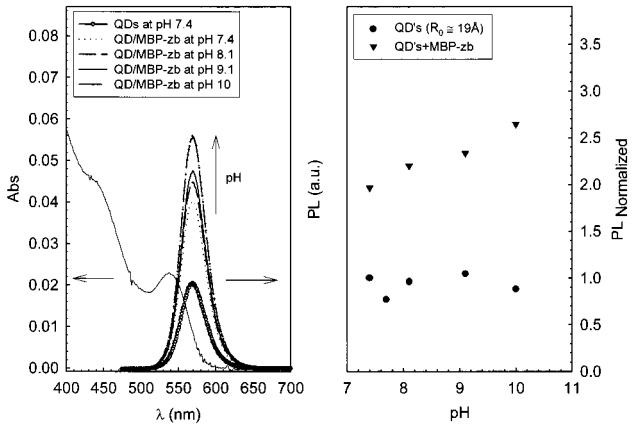

Figure 4. Left panel: Absorption and PL spectra of solutions of QDs unconjugated and conjugated with MBP-zb. Only one absorption spectrum is shown because all solutions have identical absorption spectra (same QD concentration in all samples). Right panel: Variation of the PL total integrated intensity versus solution pH for both unconjugated and QD/MBP-zb conjugates. The QD concentration was ∼150 nmol/L; the concentration of MBP-zb protein was ∼900 nmol/L (MBP-zb:QD ratio 6:1). Samples were excited at 500 nm and PL emission was measured from a 10 mm optical path length cell.

(35) Nirmal, M.; Dabbousi, B. O.; Bawendi, M. G.; Macklin, J. J.; Trautman, J. K.; Harris, T. D.; Brus, L. E. *Nature* **1996**, *383*, 802−804.
(36) Empedocles, S. A.; Neuhauser, R.; Bawendi, M. G. *Nature* **1999**, *399*, 126−130 and references therein.

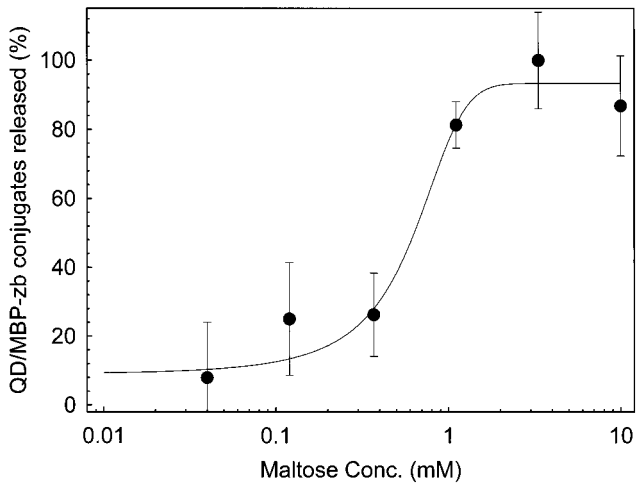

Figure 5. Release of QD/MBP-zb bioconjugates from amylose beads as a function of concentration of added maltose. Experiments were carried out in 5 mM sodium borate at pH 9. The line represents the mathematical fit to a 3-parameter sigmoid function. Such a fit is often used to account for the effects of competitive binding in titration assays.

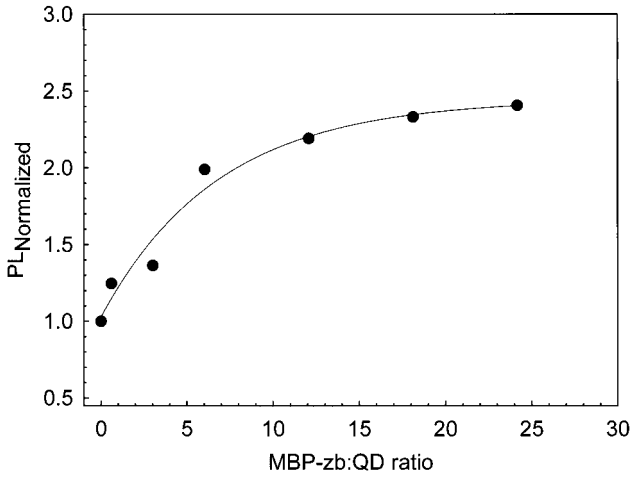

Figure 6. PL enhancement occurring upon bioconjugate formation at increasing MBP-zb:QD ratios (data normalized against unconjugated QDs). Experiments were carried out in a 5 mM sodium borate buffer solution at pH 9.

Figure 4 shows absorption and PL spectra of unconjugated nanoparticles along with QD/MBP-zb conjugates dispersed in buffered solutions at pH 7.4, 8.1, 9.1, and 10. Figure 4 also shows the PL intensity for samples containing QD/MBP-zb bioconjugates normalized to that of unconjugated QD suspensions over the same pH range. The QD/protein conjugate material retains the spectroscopic properties of the starting nanocrystals with respect to light absorption and photoluminescence. Interestingly, the data also show that conjugating these QDs with MBP-zb enhances the PL emission in comparison with that of unconjugated nanoparticles, with a somewhat more pronounced relative enhancement measured at higher pH. The PL quantum yield, as compared to the emission from a Rhodamine 6G standard in methanol, increased from ∼10% for unconjugated CdSe−ZnS QDs to ∼20−30% for CdSe−ZnS QD/MBP-zb bioconjugates.

The QD/MBP-zb bioinorganic conjugates preserve the functional properties of MBP, i.e., binding to amylose affinity resin and displacement from the resin by soluble maltose. This was qualitatively demonstrated by applying a sample of QD/MBP-zb conjugates to the top of a small chromatography column filled with amylose affinity resin. Visually observing nanoparticle PL emission (using a hand-held UV lamp for excitation) showed that essentially 100% of the QD/MBP-zb conjugates were bound to the top portion of the amylose column matrix, as indicated by a well-defined immobile narrow luminescent band. Washing the loaded column with 5 mM borate buffer did not affect the location or intensity of the conjugate band, indicating that the QD/MBP-zb conjugates retained the functions of the QD (photoluminescence) and the MBP protein domain (i.e, binding to amylose). When the column was treated with 10 mM maltose, a concentration high enough to competitively displace MBP from the affinity matrix, essentially all the luminescent material was immediately eluted, a result that confirms the efficient conjugation and preservation of biological function of the MBP protein in the present QD/MBP-zb conjugates.

The binding activity of the QD/MBP-zb bioconjugates was further explored by means of a quantitative displacement titration in a microtiter plate, once again using displacement of amylose bound conjugates by maltose. Figure 5 shows a plot of percent conjugates released as a function of maltose concentration. $K_{1/2}$, defined as the amount of maltose necessary to release ∼50% of the QD/MBP-zb conjugates at equilibrium, is approximately 0.5 mM. An increase in apparent affinity for immobilized amylose is expected due to avidity effects arising from each dot bearing several MBP-zb proteins compared with binding of free MBP and maltose (K_D = ca. 1 μM).[37] This is likely due to multiple simultaneous interactions possible with the affinity resin and quantum dots each bearing several bound proteins (see below).

Control experiments conducted under identical conditions utilizing MBP without the genetically fused charged C-terminal domain demonstrated that neither enhanced luminescence nor amylose binding occurred. This proves the importance of the designed interaction domain for formation of the QD/protein conjugates.

The above results demonstrate that effective noncovalent conjugation between these nanoparticles and MBP-zb takes place and that the new bioconjugates retain the function of the MBP domain. Figure 6 shows the relative change in the PL emission measured when the molar ratio of MBP-zb added to a fixed amount of QDs is progressively increased. The observed enhancement of PL emission (compared with that of unconjugated dots) that occurs as the protein:QD ratio is increased suggests that each QD binds multiple MBP-zb molecules. Saturation behavior occurs at a molar ratio of ca. 15−20 monomer equivalents of the protein per QD. The maximum enhancement in emission at the asymptotic plateau is ∼2.5-fold relative to unconjugated dots at the same pH. Taken together with the results of the maltose affinity titration, these studies provide additional evidence that each particle binds to several MBP-zb molecules.

Examination of the ionic strength dependence of MBP-zb quantum dot interaction by observation of changes in PL intensity of QD/MBP-zb (ca. 1/14 molar ratio) as a function of increasing NaCl concentration revealed a relatively insignificant salt dependence up to at least 1 M NaCl (Figure 7). A 2- to 2.5-fold PL intensity difference for identical numbers of unconjugated and protein-conjugated nanoparticles was maintained across the entire range of ionic strength studied.

Discussion

These experiments represent the first reported effort to conjugate lipoic acid capped quantum dots and proteins. An

(37) Miller, D. M., III; Olson, J. S.; Pflugrath, J. W.; Quiocho, F. A. *J. Biol. Chem.* **1983**, *258*, 13665−13672.

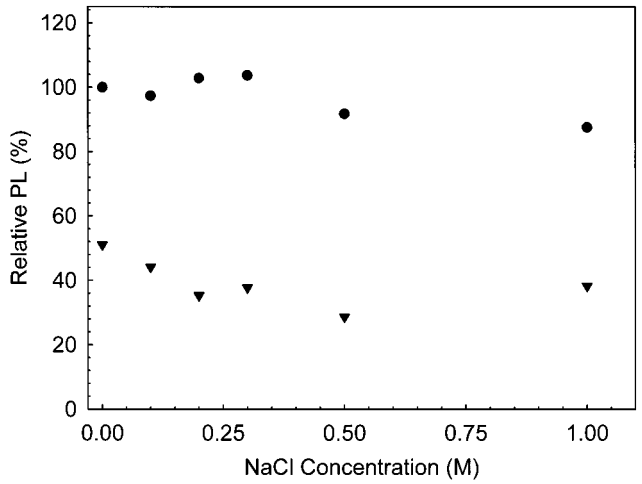

Figure 7. Effect of increasing ionic strength on the photoluminescence of CdSe−ZnS QD/MBP-zb conjugates (circles: ●) and unconjugated QDs (triangles: ▼). Samples of QD and QD/MBP-zb conjugates at pH 9, containing equal amounts of QDs, were placed into microtiter wells containing an identical volume of sodium chloride at various concentrations. The resulting photoluminescence at each salt concentration was measured in triplicate and average values were used. The PL emission from the conjugate suspension with no added NaCl was set as the reference at 100%.

advantage of the present capping is that the bidentate dihydrolipoic acid (Figure 2a) can make simultaneous capping attachment to two surface sites on the ZnS overcoating shell, theoretically resulting in more stable cap/shell interactions.[5,6] The reason for our inability to carry out the published EDC cross-linking method without formation of large amounts of macroscopic nanoparticle−protein aggregates using nanoparticles capped with lipoate groups is unknown. However, surface passivation achieved using this capping chemistry may result in a smaller density of capping groups per unit area in comparison with monothiol capping molecules.[4−6] Differences in surface properties for lipoic acid capped dots compared with monothiol capped dots may significantly alter conditions necessary for effective protein conjugation.

The present self-assembled QD/protein bioconjugates are fundamentally different from the covalent QD/protein conjugates previously described.[26,27,29] These studies illustrate the feasibility of conjugate formation due to electrostatic interactions between negatively charged lipoic-acid-capped CdSe−ZnS QDs and a specifically designed recombinant fusion protein bearing a positively charged interaction domain. Electrostatic interactions between oppositely charged polyelectrolytes have been used to self-assemble layer-by-layer thin polymeric films of various complex structures.[38,39] The layer-by-layer sequential adsorption approach was further extended to inorganic nanoparticles, dyes, and biological molecules,[40−42] and has been used to fabricate light emitting as well as photovoltaic devices.[11,12,43,44]

Design of the modular Maltose Binding Protein-basic leucine zipper (MBP-zb) fusion protein was modeled after the results of two prior published studies. Blondel and Bedouelle[45] previously demonstrated formation of bacterially produced dimeric MBP derivatives by genetically grafting the leucine zipper sequence from the yeast transcription factor GCN4 onto the C-terminus of *E. coli* MBP. We similarly connected, by means of an intervening flexible polypeptide linker, a leucine zipper sequence onto the MBP C-terminus. In the present case, we employed a highly positively charged leucine zipper designed and characterized previously by O'Shea et al.[34] to achieve oriented dimer formation by means of parallel helical coiled-coil interactions. At the most simple design level, this positively charged appended interaction domain was chosen to permit electrostatically driven self-assembly of lipoic acid capped CdSe−ZnS nanocrystal/protein conjugates.

Structural and thermodynamic measurements made by O'Shea et al.[34] have shown that parallel coiled-coil homodimer formation between the basic leucine zipper peptide domains used in the present fusion protein occurs, albeit at high concentrations (K_D of ca. 1 mM) compared with formation of heterodimers assembled from oppositely charged zipper domains (K_D of ca. 50 nM). Engineering a sterically innocuous cysteine residue just upstream of the C-terminal leucine zipper domain in the MBP-zb protein (Figure 2b) resulted in covalent homodimer formation in preparations of the purified protein under mildly oxidizing conditions. The effective increase in local peptide chain concentration achieved by covalent S−S linkage ensures concentration independent oriented homodimer formation. This feature simplifies conjugation and may assist in achieving a uniform distribution of protein complexes on negatively charged QD surfaces. In addition, formation of these S−S linked homodimeric complexes results in packing of a large amount of positive charge into a relatively small region at the C-terminus of the protein, with lysine residues constituting 22 out of 70 residues that make up the C-terminus of the protein dimer (11 lysines per 35 residue monomers). Binding to the negatively charged lipoate-modified nanoparticle surface likely relieves some of the intramolecular charge−charge repulsions occurring in this region of the dimeric C-terminal interaction domain, which in turn drives the present self-assembled conjugation process toward completion. Enhancement of electrostatic interactions by this type of structurally modulated charge neutralization can also be applied to other charged surfaces such as metallic or polymeric colloidal particles or even negatively charged natural bioassemblies such as bacteriophage.[46] Other types of interaction domains, such as those consisting of simple stretches of polylysines or polyarginines, may be effective in this role as well.[47]

An unexpected and intriguing finding of the present work is the enhancement of PL efficiency that occurs when the engineered modular MBP-zb proteins interact with the alkyl-COOH capped quantum dots in aqueous solution. It seems reasonable to speculate that surface charge neutralization that occurs as a result of the self-assembly process alters the gross electrostatic/polar environment of the inorganic core. This difference in electrostatics likely in turn affects the efficiency of core electron−hole recombination leading to the observed effect on the overall PL intensity. The pH dependence of the luminescence output acquired by the quantum dots upon conjugation with the recombinant proteins may also be an electrostatically driven phenomenon. Previous work by Spanhel

(38) Decher, G. *Science* **1997**, *277*, 1232−1237.
(39) Yoo, D.; Shiratori, S. S.; Rubner, M. F. *Macromolecules* **1998**, *31*, 4309−4318.
(40) Ariga, K.; Lvov, Y.; Kunitake, T. *J. Am. Chem. Soc.* **1997**, *119*, 2224−2231.
(41) Caruso, F.; Möhwald, H. *J. Am. Chem. Soc.* **1999**, *121*, 3039−3046.
(42) Tedeschi, C.; Caruso, F.; Möhwald, H.; Kirstein, S. *J. Am. Chem. Soc.* **2000**, *122*, 5841−5848 and references therein.
(43) Fou, A. C.; Onitsuka, O.; Ferreira, M.; Rubner, M. F.; Hsieh, B. R. *J. Appl. Phys.* **1996**, *79*, 7501−7509.
(44) Mattoussi, H.; Rubner, M. F.; Zhou, F.; Kumar, J.; Tripathy, S. K.; Chiang, L. Y. *Appl. Phys. Lett.* **2000**, *77*, 1540−1542.
(45) Blondel, A.; Bedouelle, H. *Protein Eng.* **1991**, *4*, 457−461.
(46) Mauro, J. M. Unpublished results.
(47) Nock, S.; Spudich, J. A.; Wagner, P. *FEBS. Lett.* **1997**, *414*, 233−238.

et al.[48] showed that variation in solution pH between 6.0 and 10.0 during growth of CdS nanocrystals had substantial effects on size distribution, quality (resolution) of absorption spectra, PL spectral width, and quantum yield of the final product. They attributed their observations to pH-linked changes in surface passivation occurring upon removal of dangling −SH groups on the particle surfaces. On the other hand, the present CdSe−ZnS core−shell QDs were prepared, purified, capped, and dispersed in aqueous media prior to bioconjugation, and we do not see any effects due to bioconjugation on absorption spectra or width of emission bands. It therefore seems unlikely that the spectral effects observed in both cases have the same physical origins. Elucidation of the causes of these phenomena will require further examination of the PL properties of unconjugated and charge-neutralized QD complexes.

The self-assembly of the modular MBP-zb proteins around a CdSe−ZnS nanocrystal (to form the bioconjugate) has an additional benefit to QD stability in aqueous environment. Neutralized QDs have very limited solubility in water, and lipoic acid capped CdSe−ZnS QDs precipitate out of the solution at pH < 6 (acid solutions). However, neutralized QD/protein conjugates are stable and have a higher PL quantum yield compared to unconjugated nanocrystals.

The relative lack of ionic strength dependence of the nanoparticle/protein interaction suggests that these assemblies may ultimately be stabilized to a large degree by hydrophobic interactions occurring between the nonpolar "core" residues of the fused C-terminal basic leucine zipper domain and the hydrocarbon segments of the dihydrolipoic acid capping groups. Heptad motifs of leucine residues, such as the one that exists in the basic leucine zipper domain employed here, have been shown to self-assemble within membranes and detergent solutions.[49] It is possible that the lipoic acid capped QD surface mimics to some degree a detergent micelle in its interactions with the leucine zipper of MBP-zb. Additional fundamental work aimed at probing the mechanism of formation and final structure of these materials, particularly with regard to changes in conformation of the basic leucine zipper coiled-coil domain as it interacts with the nanoparticle surface, is being pursued. Finally, the ability of these inorganic/bioorganic conjugates to remain assembled over a wide range of salt concentrations bodes well for the use of this conjugation approach in developing new biotechnological applications for quantum dot nanocrystals.

Measuring the enhancement of photoluminescence that occurs upon binding of increasing amounts of MBP-zb to a fixed amount of lipoic acid capped CdSe−ZnS QDs indicates that the self-assembly process yields bioconjugates in which each luminescent nanocrystal is surrounded by several protein molecules. The number of MBP-zb proteins than can ultimately be attached to a single QD depends on the relative sizes of the QD particle compared with the protein and possibly the conformation of the protein as it interacts with the capped nanoparticle surface as well. An estimate of the theoretical number of MBP-zb proteins that can be packed around an overcoated spherical nanocrystal can be derived from steric considerations using the expression:

$$N_{\mathrm{MBP-zb}} = 0.65\left(\frac{(R_2^{\,3} - R_1^{\,3})}{R_p^{\,3}}\right) \qquad (1)$$

where R_1 is the core−shell nanocrystal radius (without the lipoic acid cap) and $R_2 \sim R_1 + 2R_p$ is the radius of the core−shell QD plus bound MBP-zb molecules. In this model, we assume that MBP-zb molecules are close-packed as spheres around a central QD, and the C-terminal charged leucine zipper domain and flexible linker are considered to have no steric effect on packing due to their flexible conformation and relatively small size. Equation 1 takes account of the filling factor of hard spheres and adjusts the volume ratios by a factor of 0.65.[50] Using the values $R_1 = R_0 + \mathrm{d(ZnS)} \sim 30$ Å and $R_2 \sim 80$ Å ($R_p \cong 25$ Å),[51] an estimate of $N_{\mathrm{MBP-zb}} \sim 19$ per nanocrystal is derived. This estimate compares well with the experimental value derived from the PL titration data shown in Figure 6. Nonetheless, this number is subject to a slight error since crystallographic data indicate that MBP macromolecules are rather ellipsoidal in shape.[51]

The present approach has also successfully been used to modify the immunoglobulin (IgG)-binding B domain of streptococcal protein G (PG) with the same C-terminal leucine zipper peptide to prepare QD/PG-zb conjugates. We are investigating the use of these QD/PG-zb bioconjugates in fluoroimmunoassays; these results will be presented in a future report. In PG-zb, the oriented parallel coiled-coil dimeric nature of the S−S linked proteins may enhance stability of higher order QD/PG-zb/IgG conjugates due to the possibility of simultaneous two-site interaction with the F_c region of immunoglobulin G (IgG).

Conclusion

The present noncovalent self-assembly approach used to conjugate CdSe−ZnS core−shell quantum dots with recombinant fusion proteins extends and complements existing QD labeling methods. Conjugate preparation is easily achieved once the required surface-charged nanoparticles and engineered recombinant proteins have been prepared. In cases where preparation of a recombinant version of a protein bearing an appended anchor domain is impossible, purified proteins from natural sources (i.e. nonrecombinant) could be carefully labeled with charged peptides for subsequent use in QD conjugation. A strategy such as the one employed by Plank et al.[52] for electrostatically conjugating human transferrin with DNA would likely be feasible.

This electrostatic assembly approach will likely be subject to limitations in some cases. Presence of a charged interaction domain may have deleterious effects on the structure or function of an attached functional element. Furthermore, although water compatible quantum dots capped with polar but neutral groups may potentially have superior physical or photoluminescent properties, the present self-assembly method is limited to nanocrystals with charged surfaces.

The self-assembled conjugation approach described here can undoubtedly be applied to a number of different core−shell nanoparticle systems and also extended to labeling of additional types of capped size-tunable semiconductor nanomaterials and other inorganic colloidal particles, resulting in an array of bioconjugates with various useful properties. Employing other variants of engineered recombinant proteins for conjugation with luminescent quantum dots should permit considerable latitude in desired characteristics of the charged interaction domain (e.g.,

(48) Spanhel, L.; Haase, M.; Weller, H.; Hanglein, A. *J. Am. Chem. Soc.* **1987**, *109*, 5644−5649.

(49) Gurezka, R.; Laage, R.; Brosig, B.; Langosch, D. *J. Biol. Chem.* **1999**, *274*, 9265−9270 and references therein.

(50) Cebula, J.; Ottewill, R. H.; Ralston, J.; Pusey, P. N. *J. Chem. Soc., Faraday Trans.* **1981**, *I77*, 2585−2612.

(51) Spurlino, J. C.; Lu, G. Y.; Quiocho, F. A. *J. Biol. Chem.* **1991**, *266*, 5202−5219.

(52) Plank, C.; Tang, M. X.; Wolfe, A. R.; Szoka, F. C., Jr. *Hum. Gene Ther.* **1999**, *10*, 319−332.

total charge and composition, pH, and temperature stability) as well as the identity and function of the fused "bioactive" domain or domains. Furthermore, other combinations of interaction domain types and surface-charged QDs, for example negatively charged interaction domains binding to positively charged nanoparticles, should be possible. Some potential applications for these new types of nanocrystal/protein conjugates include use as sensitive detection reagents, use in cell surface labeling and intracellular tracking studies, and use for a variety of other imaging applications.

Acknowledgment. We thank Dr. S. O'Connor for assistance with the laser scanning confocal imaging and Drs. F. Ligler, B. Justus, and A. Huston at NRL for the stimulating discussions. We thank Dr. K. Ward at the Office of the Naval Research (ONR) for financial support (grants N0001499WX30470 and N0001400WX20094). This work was also funded in part by the NSF-Materials Research Science and Engineering Center program at MIT (DMR-980841).

JA002535Y